2008 IEEE International Conference on
Robotics and Automation
Pasadena, CA, USA, May 19-23, 2008

Investigation of Human-Robot Interaction Stability Using Lyapunov Theory

Vincent Duchaine and Clément M. Gosselin

Abstract— **For human-robot cooperation in the context of human-augmentation tasks, the stability of the control model is of great concern due to the risk for the human safety represented by a powerful robot. This paper investigates stability conditions for impedance control in this cooperative context and where touch is used as the sense of interaction. The proposed analysis takes into account human arm and robot physical characteristics, which are first investigated. Then, a global system model including noise filtering and impedance control is defined in a state-space representation. From this representation, a Lyapunov function candidate has been successfully discovered. In addition to providing conclusions on the global asymptotic stability of the system, the relative simplicity of the resulting equation allows the derivation of general expressions for the critical values of impedance parameters. Such knowledge is of great interest in the context of design of new adaptive control laws or simply to serve as design guidelines for conventional impedance control. The accuracy of these results were verified in a user study involving 7 human subjects and a 3-dof parallel robot. In this experiment, the real effective stability frontier was defined for each subject and compared with values predicted using the Lyapunov function.**

I. INTRODUCTION

Robots having the faculty to assist and interact with human beings have been for a long time strictly a subject of science-fiction. However, thanks to the recent drastic increase in computing power of microprocessor units and also to the commercial availability of new low-cost sensor technologies, human robot cooperation (HRC) is now an emerging field. One of the main requirements to build robots with such capabilities is that they could understand the intentions of humans and act in accordance to them. Using the sense of touch as the medium of interaction, this challenge is related to the general problem of control of constrained motion.

This problem has been well known for a few decades in robotics and many different control schemes have already been proposed. Among the schemes that satisfy HRC task requirements, the control algorithm that is probably the most commonly used is the so called impedance control [1]. However, like almost all the proposed algorithms for the control of constrained motion, this scheme is known to become unstable when facing a stiff environment [2]. Many studies cover this issue for impedance control in a general task perspective [2], [3], but very few cover this subject in the context of HRC.

This work was supported by The Natural Sciences and Engineering Research Council of Canada (NSERC) as well as by the Canada Research Chair Program, the Fonds Quebecois de Recherche sur la Nature et les Technologies (FQRNT) and General Motors (GM) Canada.

The authors are with the Departement of Mechanical Engineering, Université Laval, Québec, Québec. Canada, G1K 7P4, vincent.duchaine.1@ulaval.ca, gosselin@gmc.ulaval.ca

Having a good understanding of the stability limit of the control algorithm is fundamental for human safety when the latter are physically involved in a robot task. Due to its mechanical power, an unstable robot could severely injure a human being or even cause a fatal accident. From a control design point of view, this knowledge could also lead to design guidelines that could be helpful for developing new adaptive control laws that would no longer be a mere compromise between performance and stability.

Kazerooni in [4] defined general conditions for stability using the small gain theorem for *extender* (i.e., a class of robot manipulator worn by humans to increase human mechanical strength). The author particularly points out the trade-off that needs to be made in the design of such systems between stability of the closed-loop system and the dynamic performance. Later, in [5] Tsumugiwa et al. proposed to investigate the stability of the impedance control scheme in the context of HRC by a root locus analysis using pole locations of the characteristic equation. However, no experimentation was conducted with human subjects executing cooperative task to validate the approach. Moreover, the mathematical complexity of the approach did not allow the inference of general formulation for stability frontiers, and hence a computer solving algorithm is needed for each new designed system.

This paper presents a new analysis of the stability of impedance control for human-robot interaction based on Lyapunov stability theory. The relative simplicity of the resulting equation allows to define analytically the stability frontier as well as the critical value for each impedance parameter. The global system including both physical parts of the interaction, is first modeled. Then, a Lyapunov function candidate to the closed loop system is found. Using this function, stability frontiers and critical values of each impedance parameter are defined. Finally, assumptions made during the modelling of human and robot physical characteristics and stability results are verified in different series of experiments involving 7 human subjects.

II. MODELLING

A. Model of the physical characteristics of the human arm

In [5] only the stiffness of the arm and a delay associated with the human reaction were taken into account as human characteristics in the study of HRC stability. Obviously, stiffness is a very important property of the physical characteristics of the arm. However, damping effects and hand soft tissues also have a considerable impact on the interaction stability for HRC using the sense of touch.

1) stiffness: The human arm has a very dominant spring like characteristic that we all learn to control at an early age and that allows us to perform very dextrous movements and tasks. This stiffness greatly depends on the spatial configuration of the arm but also varies with time as a result of the activation level in bi-articulate muscles. The stiffness matrix is well known to give an ellipsoid shape distribution of the human Cartesian stiffness. For a given configuration, only the size but not the orientation of this ellipse can be modified by the level of cocontraction [6].

2) Damping: The natural viscous properties inherent to human muscles has been demonstrated [7] to be of great importance in the stabilization of human movements thanks to the role that they play in disturbance rejection.

As seen in the preceding paragraph, humans have the natural ability to adjust the stiffness of their arms using different activation levels in antagonistic and agonistic muscles. Some studies [8], [9] have shown that viscosity properties of the arm also simultaneously increase or decrease with the stiffness variation. The investigation of the relationship between these two characteristics in [9], [10] led to the conclusion that the damping ratio is constant regardless of bi-articulate muscle activation level. This fact gives a direct relation between the damping effect and the square root of the stiffness.

According to these results the human arm damping effect in each Cartesian direction will be modelled here, using the following equation:

$$d = \alpha\sqrt{k_h} \tag{1}$$

where d is the damping coefficient, k_h is the stiffness in the corresponding direction and α is a weighting factor. The analysis of the Cartesian space data obtained in the human cooperation study of [11] also supports this relationship.

3) Hand Soft Tissue Properties: Human-robot cooperation using touch as the medium of interaction involves also the effect of the superposed hand skin, fat and muscle elasticity properties since the interaction is made via this part. Because of its very short limited range of compression, this elasticity property cannot simply be added in series with the elasticity of the arm.

Around the origin and with other initial conditions close to zero, the stiffness of the skin alone can be sufficient to define stability of the interaction, since for these conditions the equivalent stiffness of the whole system is roughly equal to the stiffness of the skin. This human soft contact property is very important for grasping stability. However, the use of this stiffness alone could not guarantee stability for all state vector values. For some given state values the skin can reach its maximum compressibility and then, the global stiffness could shift to the one of the arm. Since such perturbations or conditions will always happen in a real implementation, the effect of the skin will be neglected in the human model with the consequences that for some very low state values, the critical stability frontier could be slightly overshot. Moreover, to the best knowledge of the authors, the properties of the hand soft tissue are well covered in the literature but not in a way that could be useful in this context. Therefore, it could be difficult to take into account this characteristic in the model.

B. Robot model

It may appear useless to consider the robot stiffness since the latter is often very high, and its effect on the coupled stiffness is almost negligible. This statement is true for most current robots. However, there is a strong design effort at this moment to build a new generation of human-safe robots with low impedance and some compliance. In this case, the complete stiffness of the robot may have a considerable impact on the coupled stiffness with positive repercussions on the global stability of the system.

In most cases, robot links are a lot stiffer than the actuators. Under this assumption, the robot stiffness can be represented by the stiffness of its actuator. Starting with the well-known relation:

$$\boldsymbol{\tau} = \mathbf{J}_q^T\mathbf{F} \tag{2}$$

where $\boldsymbol{\tau}$ is the vector of joint torques, $\mathbf{J}_q$ is the Jacobian matrix of the robot and $\mathbf{F}$ is the vector of cartesian forces/torques. We can relate the joint stiffness ($\mathbf{K}_q$) to the Cartesian one ($\mathbf{K}_x$) using the derivation proposed by Chen and Kao [12]. Following this, eq. (2)can be differentiated to yield:

$$d\boldsymbol{\tau} = (d\mathbf{J}_q^T)\mathbf{F} + \mathbf{J}_q^T(d\mathbf{F}) \tag{3}$$

Using the definition of stiffness, this equation can be rearranged as:

$$\mathbf{J}_q^T\mathbf{K}_x d\mathbf{x} = \mathbf{K}_q d\mathbf{q} - \left(\frac{\partial \mathbf{J}_q^T}{\partial \mathbf{q}} d\mathbf{q}\right)\mathbf{F} \tag{4}$$

where $\mathbf{q}$ and $\mathbf{x}$ are respectively joint and Cartesian coordinate vectors. With the use of the relation:

$$d\mathbf{x} = \mathbf{J}_q d\mathbf{q}, \tag{5}$$

the expression of the Cartesian stiffness matrix of the manipulator becomes:

$$\mathbf{K}_x = \mathbf{J}_q^{-T}\left(\mathbf{K}_q - \frac{\partial \mathbf{J}_q^T}{\partial \mathbf{q}}\mathbf{F}\right)\mathbf{J}_q^{-1}. \tag{6}$$

Hence, under the assumption of a high structural stiffness we have:

$$\mathbf{K}_r = \mathbf{K}_x \tag{7}$$

where $\mathbf{K}_r$ is the stiffness matrix of the robot. If the robot is designed with the objective of a low inertia and the links have a relatively low stiffness— like sometimes with parallel robots— the structural stiffness should be considered. For this case, the global robot stiffness matrix become:

$$\mathbf{K}_r = \left(\mathbf{K}_x + \mathbf{K}_s\right)^{-1}\mathbf{K}_x\mathbf{K}_s \tag{8}$$

where $\mathbf{K}_s$ is the structural stiffness of the links. Sometimes, in human robot cooperative tasks, the interaction does not

directly happen between the robot and the human but via an object held in cooperation. For this case, the object should be considered as a structural extension of the robot.

C. Coupled stiffness

Since the human and the robot are directly in constant contact during the interaction, the effective stiffness $\mathbf{K}_{eff}$ of the coupled system is given by:

$$\mathbf{K}_{eff} = (\mathbf{K}_h + \mathbf{K}_r)^{-1} \mathbf{K}_h \mathbf{K}_r \tag{9}$$

where $\mathbf{K}_h$ and $\mathbf{K}_r$ are respectively the human and robot Cartesian stiffness, as defined in the above sections.

D. Model of Impedance Control scheme

In the present analysis, the dynamics of the robot will be modelled as its given impedance characteristics. The general impedance equation can be represented as:

$$\mathbf{F} = m\ddot{\mathbf{x}} + c\dot{\mathbf{x}} + k\mathbf{x} \tag{10}$$

where $\mathbf{F}$ is the force vector, $\mathbf{x}$ the displacement vector and m, c and k are the mass, damping and stiffness parameters. However, in HRC, virtual stiffness is often set to zero since this parameter can become an obstacle for carrying tasks [1]. The impedance equation is then reduced to:

$$\mathbf{F} = m\ddot{\mathbf{x}} + c\dot{\mathbf{x}}. \tag{11}$$

Typically, impedance control in HRC implies the use of a force sensor. Such a sensor is often very noisy and requires in most cases the use of a filter. The use of a filter has a major impact on the stability since it induces delays in the feedback. A first order filter will be assumed in the model. Such a simple filter is probably the most commonly used. The transfer function for this filter G_f is:

$$G_F(s) = \frac{1}{Ts + 1} \tag{12}$$

where T is the time constant of the filter.

Even if robot controllers always run in a discrete mode with the consequence of a delay equal to the sampling period, the servo rate used is commonly very high. The effect of the sampling is thus marginal compared to the impact of the low dynamics of the noise filter and the impedance function. The sampling delay will therefore be neglected here. This assumption will not induce significant errors. However, if the sampling period becomes the critical delay in the system, it should be considered.

Since the human and the robot are rigidly in contact, the Cartesian position is assumed to be the same as the one of the robot. Figure 1 gives a schematic representation of the model including the human. Combining the impedance model and the filter leads to a third order function that can be represented in state space by the following system of equations:

$$\begin{aligned} \dot{x}_1 &= x_2 \\ \dot{x}_2 &= x_3 \\ \dot{x}_3 &= \frac{F - (m + cT)x_3 - cx_2}{mT} \end{aligned} \tag{13}$$

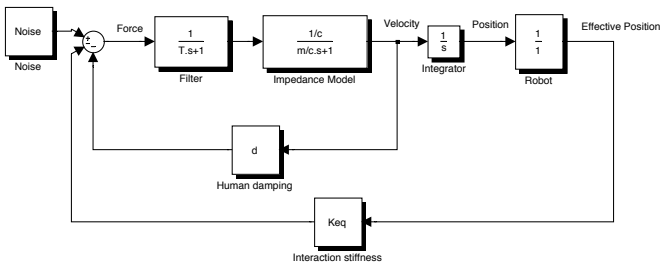

Fig. 1. Representation of the system.

where x_1, x_2 and x_3 are the state variables. Assuming that the human operator is in direct contact with the robot or with an object supported by the robot, the feedback can be written as:

$$F = -K_{eq}x_1 - dx_2 \tag{14}$$

which leads to the following closed-loop system:

$$\begin{aligned} \dot{x}_1 &= x_2 \\ \dot{x}_2 &= x_3 \\ \dot{x}_3 &= \frac{-K_{eq}x_1 - (m + cT)x_3 - (c + d)x_2}{mT}. \end{aligned} \tag{15}$$

Such a system can be represented in state space by:

$$\dot{\mathbf{x}} = \mathbf{A}\mathbf{x} \tag{16}$$

with the following state matrix:

$$\mathbf{A} = \frac{1}{mT} \begin{bmatrix} 0 & mT & 0 \\ 0 & 0 & mT \\ -K_{eq} & -(c + d) & -(m + cT) \end{bmatrix}. \tag{17}$$

This state matrix will be used in the next section to investigate the stability condition of the control scheme.

III. Stability analysis using Lyapunov function

Since the present system is linear, we could simply look at the eigenvalues of the 3×3 state matrix to conclude on stability. However, although the characteristic polynomial is clearly simple, the expressions of the roots are not. While we can find a general analytic expression for critical impedance mass using these roots solved with the help of a computer, their complexity does not allow us to find relations for critical impedance damping, which is more a subject of interest. Using the so-called Lyapunov direct method for stability will allow some simplifications that will easily lead to such expressions.

A. Lyapunov Candidate

From the Lyapunov theorem [13] we know that if there exists a scalar function V of the state $\mathbf{x}$, with continuous first order derivatives such that

$$\begin{aligned} &V(\mathbf{x}) \text{ is positive definite} \\ &\dot{V}(\mathbf{x}) \text{ is negative definite} \\ &V(\mathbf{x}) \to \infty \text{ as } \|\mathbf{x}\| \to \infty \end{aligned}$$

then the equilibrium at the origin is globally asymptotically stable.

Starting with the general Lyapunov candidate:

$$V(\mathbf{x}) = \mathbf{x}^T\mathbf{P}\mathbf{x}, \tag{18}$$

the first condition for global stability will be fulfilled if $\mathbf{P}$ is positive definite. This function also clearly satisfies the condition of infinity for infinite state values.

The time derivative of this function can be expressed as:

$$\dot{V}(\mathbf{x}) = \dot{\mathbf{x}}^T\mathbf{P}\mathbf{x} + \mathbf{x}^T\mathbf{P}\dot{\mathbf{x}} = -2\mathbf{x}^T\mathbf{Q}\mathbf{x}. \tag{19}$$

If matrix $\mathbf{Q}$ is positive definite — with the consequence of $\dot{V}(\mathbf{x})$ being negative definite — the second condition will be satisfied and global stability of the system in the sense of Lyapunov will be guarantee. Substituting eq. (16) into eq. (19) leads to the so-called Lyapunov equation, which can be used to find a Lyapunov function candidate:

$$\mathbf{A}^T\mathbf{P} + \mathbf{P}\mathbf{A} = -2\mathbf{Q}. \tag{20}$$

For computational simplicity we will assume $\mathbf{Q} = \mathbf{I}$. This matrix is obviously a positive definite matrix. Substituting all the values into eq. (20), leads to the following matrix equation

$$\begin{bmatrix} p_{21}+p_{12}+2 & p_{22}+p_{13} & r_1 \\ p_{31}+p_{22} & p_{32}+p_{23}+2 & r_2 \\ r_1 & r_2 & r_3 \end{bmatrix} = \mathbf{0} \tag{21}$$

with

$$r_1 = \frac{p_{11}K_{eq}+(c+d)p_{12}+(m+cT)p_{13}}{-mT} + p_{23} \tag{22}$$

$$r_2 = \frac{p_{21}K_{eq}+(c+d)p_{22}+(m+cT)p_{23}}{-mT} + p_{33} \tag{23}$$

$$r_3 = \frac{(p_{13}+p_{31})K_{eq}+(c+d)(p_{23}+p_{32})+2(m+cT)p_{33}}{-mT} + 2. \tag{24}$$

The four equations given by the upper-left sub-matrix of eq. (21) can be easily solved, leading to:

$$p_{12} = p_{21} = p_{23} = p_{32} = -1 \tag{25}$$

and

$$p_{13} = p_{31} = -p_{22}. \tag{26}$$

Using these results, matrix $\mathbf{P}$ can be greatly simplified and becomes:

$$\mathbf{P} = \begin{bmatrix} p_{11} & -1 & -p_{22} \\ -1 & p_{22} & -1 \\ -p_{22} & -1 & p_{33} \end{bmatrix}. \tag{27}$$

Substituting this simplified matrix into eq. (20) gives a fully constrained system of 3 equations that can be solved easily. Solving these equations, one has

$$p_{11} = \frac{B_1m^3+B_2m^2+B_3m+B_4}{K_{eq}(-K_{eq}T+c+d)m+c^2T+cTd} \tag{28}$$

$$p_{22} = \frac{B_1m^2+(3cT+K_{eq}+Td)m+c^2T^2+kTc}{(-K_{eq}T+c+d)m+c^2T+cTd} \tag{29}$$

$$p_{33} = \frac{{K_{eq}}^2+K_{eq}(m+Tc)+c^2+2cd+d^2+mTd}{(-K_{eq}T+c+d)m+c^2T+cTd} \tag{30}$$

$$\tag{31}$$

with

$$B_1 = 1 + T^2 \tag{32}$$

$$B_2 = K_{eq} + 3cT + T^2K_{eq} \tag{33}$$

$$B_3 = K_{eq}T(c-d) + c^2 + 2cd + d^2 + 3c^2T^2 \tag{34}$$

$$B_4 = c^2T^2(K_eq + cT) + cT(c^2 + 2cd + d^2). \tag{35}$$

B. Positive definiteness of matrix $\mathbf{P}$

A necessary condition for a matrix to be positive definite is that all its diagonal entries be positive. From this statement, we can conclude that the system is unstable when p_{11}, p_{22} or p_{33} become negative. Due to their physical meaning K_{eq}, d, c and m will always be in $\Re_+$. Hence, it can be easily seen that the numerator of eqs. (29, 30, 31) will always be positive. Therefore, the only way that the diagonal elements of matrix $\mathbf{P}$ become negative is that the denominator, which is the same for all terms, becomes negative. The system is thus clearly unstable when:

$$\left((-K_{eq}T + c + d)\,m + c^2T + cTd\right) < 0 \tag{36}$$

This condition gives some indications on instability but is not *a priori* sufficient to describe if the system is stable. A necessary and sufficient condition for a matrix $\mathbf{P}_{(n\times n)}$ to be positive definite is, that all its principal minors are positive The first leading minor is given directly by coefficient p_{11}. Positiveness definition of this term results directly on the sign of eq. (36). While it can be shown that the third one is always positive, to the best knowledge of the authors it is only possible to prove that the second leading minor is positive when the first one is also positive. From this result, it follows that the necessary condition for positive definiteness is in this case sufficient and then the sign of eq. (36) can be used to conclude on the stability of the impedance control scheme in the context of HRC.

C. Critical impedance parameters

It was shown in the preceding subsection that eq. (36) is sufficient to determine when the system is globally asymptotically stable in the sense of Lyapunov. Using this low order equation, a relation giving the critical frontier for each impedance parameter can be found.

We can note that for given characteristics of the human operator (K_{eq} and d) and the filter that needs to be set, eq. (36) is linear in m. Critical mass parameters can be found when this function is equal to zero, i.e., when the system is critically stable. This equation has only one solution given by:

$$m_c = -\frac{cT\ (c+d)}{-K_{eq}T + c + d}. \tag{37}$$

Probably more important, the critical damping parameter is given by finding the roots of eq. (36) with c as a variable. Since this equation is quadratic, two roots can be found; one negative and the other almost always positive. Due to the physical meaning, critical damping will be given by the positive root, namely:

$$c_c = \frac{-(m+Td) + \sqrt{m^2 - 2mTd + (d^2 + 4K_{eq}m)T^2}}{2T}. \tag{38}$$

If this equation leads to a negative result, then the control is stable for any positive value of the damping coefficient. This can happen when the stiffness is very low. This result indicates that the closed-loop function tends to become a simple mass and damping system, which is known to have an infinity of equilibrium points.

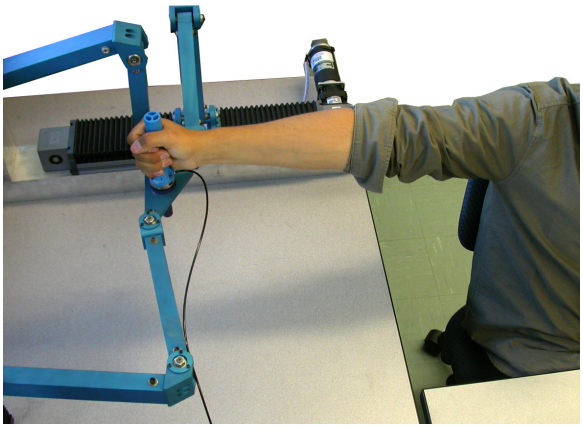

Fig. 2. Posture of the human during the interaction with the robot.

IV. Experimental Validation

A. Objective of the experiments

The stability control analysis presented in this paper aims at providing direct mathematical tools to design new control laws for HRC. Thus, this section will illustrate the capability of the method described above to predict the stability frontier for impedance control on a real cooperative system.

The first part of the experiment was conducted using a very simple fake human arm built essentially of aluminum and springs. This preliminary test was first made to help us verify the accuracy of our implementation of the Mussa-Ivaldi [6] procedure to identify stiffness, since this value is already known from the manufacturer. Also, the use of this simple system allowed us to test our conclusion on stability for impedance control without having to deal with all the uncertainties associates with a real human arm.

The next set of experiments was conducted with real human subjects interacting with a robot. The stiffness of their arms was first estimated and then the critical damping parameters were determined experimentally.

B. Experimental setup

The study was performed with the help of 7 different subjects of age ranging from 21 to 30. This group was formed of 4 males and 3 females. Five of them were right-handed and the other two were left-handed. Except for two male subjects, all of them had never interacted with a robot previously.

The robot used for this experiment, was the Tripteron [14], a 3-DOF parallel robot. This robot is a fully decoupled translational parallel manipulator and hence the Jacobian matrix is the identity matrix in all configurations and so dexterity remains constant over all the workspace. This characteristic is very useful in the context of HRC because the human operator does not have to consider the possibility of encountering a singular configuration. The use of this parallel manipulator also allows to cover a wide range of human motion in terms of acceleration and velocity since the Tripteron can perform accelerations higher than 5g. A six-axis force/torque sensor ATI mini-40 was mounted on the end-effector. In order to minimize the effect of the noise on the force sensor, a low pass filter with a time constant of 0.1125s was used. The controller is implemented on a real-time QNX computer with a sampling period of 2ms.

TABLE I

Stiffness estimation (N/m) and critical damping (Ns/m) for the simple spring human arm model

	K_h	K_h estimated	Predicted c_c	Experimental c_c
Spring 1	5500	5347	94.9	92
Spring 2	3200	3114	70.5	69
Spring 3	2500	2287	59.3	58

C. Experimentation and results

1) Fake human arm experimentation: The experimentation with the fake human arm was conducted using 3 different springs. The damping effect was neglected due to its low value. The virtual mass of the impedance model was set for this experiment to 2 kg. Table I shows the stiffness estimation results, the experimental critical damping frontier and the predicted one. It can be seen that both are very close and that in the case of low human model uncertainties, the proposed method for stability investigation adequately predicts the stability behaviour of the robot. The estimated stiffness appears to be always lower than the manufacturer's specification. However, it is recalled that this stiffness considers also the effect of the robot stiffness with the consequence of lower results.

2) Stiffness identification: Figure 2 shows the human position selected for the interaction with the robot. This position was experimentally found to give a very stiff arm behaviour in one direction. In this case, the maximum eigenvalue for the ellipse representing the stiffness matrix is clearly oriented parallel to the human arm. Such a position was used to simplify our identification test since investigation of the human arm stiffness is not the main focus of this paper. Following this, only the stiffness in this principal direction was evaluated.

As mentioned in the preceding section, stiffness characterization was implemented according to the Mussa-Ivaldi [6] procedure. The same robot was used for the arm characterization as for the interaction stability test, with the consquence of the resulting stiffness already taking into account the stiffness of the robot. This identification test, in which a human was asked to contract the muscle of their arm at their maximum level, was performed eight times and the average was taken as the stiffness value. Figure 3 shows the estimated stiffness for the 7 subjects.

3) Critical damping estimation: The values obtained in the preceding section were used to compute the estimated stability frontier for the impedance control for each subject in order to compare with experimental results. A human damping characteristic directly related to the square root of the stiffness was taken into account ($\alpha = 1$). During this experiment, the subjects were asked to keep the same position and level of muscle contraction as during the arm characterization procedure. On the robot's side, the impedance mass parameter was set to 2 kg and the damping

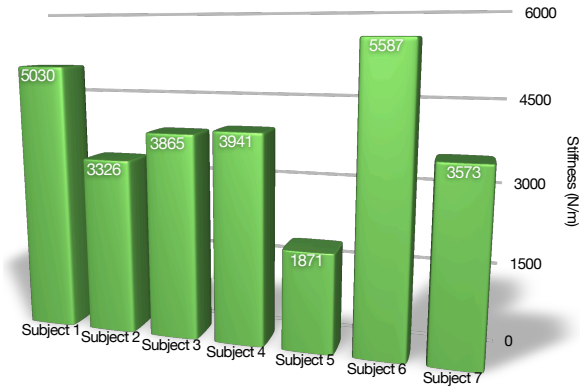

Fig. 3. Estimation of the maximum arm stiffness for each subject.

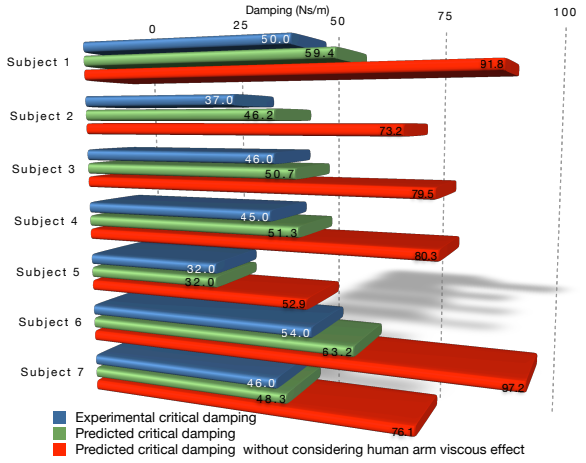

Fig. 4. Predicted and experimentally measured critically stable damping coefficient.

was initially set to 75 $\frac{Ns}{m}$. This value has been progressively lowered by increments of 1 $\frac{Ns}{m}$ until the human started to feel cooperation instability.

Since humans can only contract their muscle at a same level for a short period of time, it was important to keep the experimentation as short as possible. Therefore, only the critical damping was targeted in this experiment. Instability can obviously occur for a different value of mass parameters, depending on the rest of the system. However, the higher the mass parameter for which instability happens, the lower is the frequency of the resulting increasing oscillation. At some point the frequency is so slow that it becomes very hard for the human subject to conclude whether the control is really stable or not around the frontier. Also, experimentations in [11] showed that a fixed low mass should be targeted for HRC. Figure 4 shows both predicted and experimental critical damping parameters. Predicted results where only the stiffness is taken into account in the human model is also provided on this graph. This is to illustrate the impact of neglecting the viscous effect in the human arm, like in the stability study of [5].

It can be observed on this figure, that the method proposed in this paper is relatively good at predicting the stability frontier of the impedance control in an HRC context. However, the method appears to always slightly overestimate this frontier. This can be related to the fact that we neglect the skin softness in our model but probably more to the approximate relation we assumed for the human arm damping. Finally, the results where only stiffness has been taken into account for the human characteristics, largely overestimate the frontier.

V. Conclusion

In this study, we proposed to investigate the stability of impedance control in the context of human-robot cooperation using Lyapunov theory. A model of both human and robot characteristics was built and a Lyapunov function candidate for the whole system was found. Using the relatively simple equation obtained, we defined general stability frontiers but also critical values of each impedance parameter to serve as design guidelines. These useful tools were observed to provide accurate prediction of the stability in a real HRC context during an experimental validation, involving 7 human subjects. Future work will focus on the integration of these results to build new adaptive control laws that could guarantee global stability of the control algorithm.

References

[1] T. Tsumugiwa, R. Yokogawa, and K. Hara, "Variable impedance control based on estimation of human arm stiffness for human-robot cooperative calligraphic task," *Proc. IEEE Int. Conf. on Robotics and Automation*, pp. 644–650, 2002.

[2] D. Surdilovic, "Contact stability issues in position based impedance control: Theory and experiments," *Proceeding of the Internationnal Conference on Robotics and Automation*, vol. 4, pp. 1675–1681, 1996.

[3] D.A.Lawrence, "Impedance control stability properties in common implementations," *Proc. IEEE Int. Conf. on Robotics and Automation*, pp. 1185–1190, 1988.

[4] H. Kazerooni, "Stability and performance of human-robot interaction," *Proc. IEEE Int Conf. on Systems, Man and Cybernetics*, vol. 2, pp. 494–497, 1989.

[5] T. Tsumugiwa, R. Yokogawa, and K. Yoshida, "Stability analysis for impedance control of robot for human-robot cooperative task system," *Proc. IEEE Int Conf. on Intelligent Robots and Systems*, vol. 6, pp. 3883–3888, 2004.

[6] F. Mussa-Ivaldi, N. Hogan, and E. Bizzi, "Neural, mechanical and geometric factors subserving arm posture in humans," *J. Neuroscience*, vol. 5, pp. 2752–2743, 1985.

[7] E. Burdet, R. Osu, D. Franklin, T. Milner, and M. Kawato, "The central nervous system stabilizes unstable dynamics by learning optimal impedance.," *Nature*, vol. 414, no. 6862, pp. 446–9, 2001.

[8] H. Gomi and R. Osui, "Task-dependent viscoelasticity of human multijoint arm and its spatial characteristics for interaction with environments," *J. Neuroscience*, vol. 21, pp. 8965–8978, 1998.

[9] F. Lacquaniti, F. Licata, and J. Soechting, "The mechanical behavior of the human forearm in response to transient perturbations," *Biological Cybernetics*, vol. 44, no. 1, pp. 35–46, 1982.

[10] R. Kearney and I. Hunter, "System identification of human joint dynamics.," *Crit Rev Biomed Eng*, vol. 18, no. 1, pp. 55–87, 1990.

[11] M. Rahman, R. Ikeura, and K. Mitzutani, "Investigating the impedance characteristic of human arm for development of robots to cooperate with human operators.," *Proc. IEEE Int Conf. on Systems, Man and Cybernetics*, vol. 2, pp. 676–681, 1999.

[12] S. Chen and I. Kao, "Conservative Congruence Transformation for Joint and Cartesian Stiffness Matrices of Robotic Hands and Fingers," *The International Journal of Robotics Research*, vol. 19, no. 9, p. 835, 2000.

[13] A. Lyapunov, "The general problem of the stability of motion," *International Journal of Control*, vol. 55, no. 3, pp. 531–534, 1992.

[14] C. Gosselin, M. Masouleh, V. Duchaine, P. Richard, S. Foucault, and X. Kong, "Parallel Mechanisms of the Multipteron Family: Kinematic Architectures and Benchmarking," *Robotics and Automation, 2007 IEEE International Conference on*, pp. 555–560, 2007.